Proc. 8th Asian Conference on Computer Vision (ACCV2007)
Nomvember 2007, Tokyo, Japan, Vol. 2, pp. 311–321.

Highest Accuracy Fundamental Matrix Computation

Yasuyuki Sugaya[1] and Kenichi Kanatani[2]

[1]Department of Information and Computer Sciences,
Toyohashi University of Technology, Toyohashi, Aichi 441-8580 Japan
sugaya@iim.ics.tut.ac.jp
[2]Department of Computer Science, Okayama University, Okayama 700-8530, Japan
kanatani@suri.cs.okayama-u.ac.jp

Abstract. We compare algorithms for fundamental matrix computation, which we classify into "a posteriori correction", "internal access", and "external access". Doing experimental comparison, we show that the 7-parameter Levenberg-Marquardt (LM) search and the extended FNS (EFNS) exhibit the best performance and that additional bundle adjustment does not increase the accuracy to any noticeable degree.

1 Introduction

Computing the fundamental matrix from point correspondences is the first step of many vision applications including camera calibration, image rectification, structure from motion, and new view generation [6]. To compute the fundamental matrix accurately from noisy data, we need to solve optimization subject to the constraint that it has rank 2, for which typical approaches are:

A posteriori correction. We first compute the fundamental matrix without considering the rank constraint and then modify the solution so that it is satisfied (Fig. 1(a)).

Internal access. We minimally parameterize the fundamental matrix so that the rank constraint is always satisfied and do optimization in the reduced ("internal") parameter space (Fig. 1(b)).

External access. We do iterations in the redundant ("external") parameter space in such a way that an optimal solution that satisfies the rank constraint automatically results (Fig. 1(c)).

The aim of this paper is to find the best method by thorough performance comparison.

2 Mathematical Fundamentals

Fundamental matrix. Given two images of the same scene, a point (x, y) in the first image and the corresponding point (x', y') in the second satisfy the *epipolar equation* [6]

Y. Yagi et al. (Eds.): ACCV 2007, Part II, LNCS 4844, pp. 311–321, 2007.

$$(\begin{pmatrix} x/f_0 \\ y/f_0 \\ 1 \end{pmatrix}, \begin{pmatrix} F_{11} & F_{12} & F_{13} \\ F_{21} & F_{22} & F_{23} \\ F_{31} & F_{32} & F_{33} \end{pmatrix} \begin{pmatrix} x'/f_0 \\ y'/f_0 \\ 1 \end{pmatrix}) = 0, \tag{1}$$

where f_0 is a scaling constant for stabilizing numerical computation [5] (In our experiments, we set $f_0 = 600$ pixels). Throughout this paper, we denote the inner product of vectors $\boldsymbol{a}$ and $\boldsymbol{b}$ by $(\boldsymbol{a}, \boldsymbol{b})$. The matrix $\boldsymbol{F} = (F_{ij})$ in Eq. (1) is of rank 2 and called the *fundamental matrix*. If we define

$$\boldsymbol{u} = (F_{11}, F_{12}, F_{13}, F_{21}, F_{22}, F_{23}, F_{31}, F_{32}, F_{33})^\top, \tag{2}$$

$$\boldsymbol{\xi} = (xx', xy', xf_0, yx', yy', yf_0, f_0x', f_0y', f_0^2)^\top, \tag{3}$$

Equation (1) can be rewritten as

$$(\boldsymbol{u}, \boldsymbol{\xi}) = 0. \tag{4}$$

The magnitude of $\boldsymbol{u}$ is indeterminate, so we normalize it to $\|\boldsymbol{u}\| = 1$, which is equivalent to scaling $\boldsymbol{F}$ so that $\|\boldsymbol{F}\| = 1$. With a slight abuse of symbolism, we hereafter denote by $\det \boldsymbol{u}$ the determinant of the matrix $\boldsymbol{F}$ defined by $\boldsymbol{u}$.

Covariance matrices. Given N observed noisy correspondence pairs, we represent them as 9-D vectors $\{\boldsymbol{\xi}_\alpha\}$ in the form of Eq. (3) and write $\boldsymbol{\xi}_\alpha = \bar{\boldsymbol{\xi}}_\alpha + \Delta\boldsymbol{\xi}_\alpha$, where $\bar{\boldsymbol{\xi}}_\alpha$ is the true value and $\Delta\boldsymbol{\xi}_\alpha$ the noise term. The covariance matrix of $\boldsymbol{\xi}_\alpha$ is defined by

$$V[\boldsymbol{\xi}_\alpha] = E[\Delta\boldsymbol{\xi}_\alpha \Delta\boldsymbol{\xi}_\alpha^\top], \tag{5}$$

where $E[\,\cdot\,]$ denotes expectation over the noise distribution. If the noise in the x- and y-coordinates is independent and of mean 0 and standard deviation σ, the covariance matrix of $\boldsymbol{\xi}_\alpha$ has the form $V[\boldsymbol{\xi}_\alpha] = \sigma^2 V_0[\boldsymbol{\xi}_\alpha]$ up to $O(\sigma^4)$, where

$$V_0[\boldsymbol{\xi}_\alpha] = \begin{pmatrix} \bar{x}_\alpha^2 + \bar{x}_\alpha'^2 & \bar{x}'_\alpha\bar{y}'_\alpha & f_0\bar{x}'_\alpha & \bar{x}_\alpha\bar{y}_\alpha & 0 & 0 & f_0\bar{x}_\alpha & 0 & 0 \\ \bar{x}'_\alpha\bar{y}'_\alpha & \bar{x}_\alpha^2 + \bar{y}_\alpha'^2 & f_0\bar{y}'_\alpha & 0 & \bar{x}_\alpha\bar{y}_\alpha & 0 & 0 & f_0\bar{x}_\alpha & 0 \\ f_0\bar{x}'_\alpha & f_0\bar{y}'_\alpha & f_0^2 & 0 & 0 & 0 & 0 & 0 & 0 \\ \bar{x}_\alpha\bar{y}_\alpha & 0 & 0 & \bar{y}_\alpha^2 + \bar{x}_\alpha'^2 & \bar{x}'_\alpha\bar{y}'_\alpha & f_0\bar{x}'_\alpha & f_0\bar{y}_\alpha & 0 & 0 \\ 0 & \bar{x}_\alpha\bar{y}_\alpha & 0 & \bar{x}'_\alpha\bar{y}'_\alpha & \bar{y}_\alpha^2 + \bar{y}_\alpha'^2 & f_0\bar{y}'_\alpha & 0 & f_0\bar{y}_\alpha & 0 \\ 0 & 0 & 0 & f_0\bar{x}'_\alpha & f_0\bar{y}'_\alpha & f_0^2 & 0 & 0 & 0 \\ f_0\bar{x}_\alpha & 0 & 0 & f_0\bar{y}_\alpha & 0 & 0 & f_0^2 & 0 & 0 \\ 0 & f_0\bar{x}_\alpha & 0 & 0 & f_0\bar{y}_\alpha & 0 & 0 & f_0^2 & 0 \\ 0 & 0 & 0 & 0 & 0 & 0 & 0 & 0 & 0 \end{pmatrix}. \tag{6}$$

In actual computations, the true positions $(\bar{x}_\alpha, \bar{y}_\alpha)$ and $(\bar{x}'_\alpha, \bar{y}'_\alpha)$ are replaced by their data (x_α, y_α) and (x'_α, y'_α), respectively.

We define the covariance matrix $V[\hat{\boldsymbol{u}}]$ of the resulting estimate $\hat{\boldsymbol{u}}$ of $\boldsymbol{u}$ by

$$V[\hat{\boldsymbol{u}}] = E[(\boldsymbol{P}_{\mathcal{U}}\hat{\boldsymbol{u}})(\boldsymbol{P}_{\mathcal{U}}\hat{\boldsymbol{u}})^\top], \tag{7}$$

where $\boldsymbol{P}_{\mathcal{U}}$ is the linear operator projecting $\mathcal{R}^9$ onto the domain $\mathcal{U}$ of $\boldsymbol{u}$ defined by the constraints $\|\boldsymbol{u}\| = 1$ and $\det \boldsymbol{u} = 0$; we evaluate the error of $\hat{\boldsymbol{u}}$ by projecting it onto the tangent space $T_{\boldsymbol{u}}(\mathcal{U})$ to $\mathcal{U}$ at $\boldsymbol{u}$.

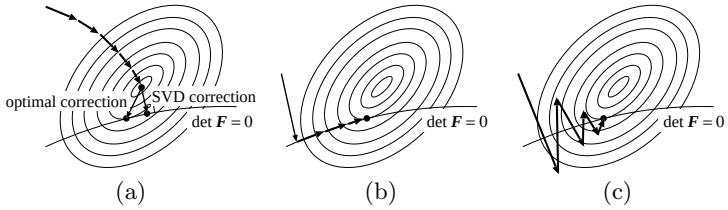

Fig. 1. (a) A posteriori correction. (b) Internal access. (c) External access.

Geometry of the constraint. The unit normal to the hypersurface defined by $\det \boldsymbol{u} = 0$ is

$$\boldsymbol{u}^\dagger = N[\nabla_{\boldsymbol{u}} \det \boldsymbol{u}], \tag{8}$$

where $N[\,\cdot\,]$ denotes normalization into unit norm. It is easily shown that the constraint $\det \boldsymbol{u} = 0$ is equivalently written as

$$(\boldsymbol{u}^\dagger, \boldsymbol{u}) = 0. \tag{9}$$

Since the domain $\mathcal{U}$ is included in the unit sphere $\mathcal{S}^8 \subset \mathcal{R}^9$, the vector $\boldsymbol{u}$ is everywhere orthogonal to $\mathcal{U}$. Hence, $\{\boldsymbol{u},\ \boldsymbol{u}^\dagger\}$ is an orthonormal basis of the orthogonal complement of the tangent space $T_{\boldsymbol{u}}(\mathcal{U})$. It follows that the projection operator $\boldsymbol{P}_{\mathcal{U}}$ in Eq. (7) has the following matrix representation:

$$\boldsymbol{P}_{\mathcal{U}} = \boldsymbol{I} - \boldsymbol{u}\boldsymbol{u}^\top - \boldsymbol{u}^\dagger \boldsymbol{u}^{\dagger\top}. \tag{10}$$

KCR lower bound. If the noise in $\{\boldsymbol{\xi}_\alpha\}$ is independent and Gaussian with mean $\boldsymbol{0}$ and covariance matrix $\sigma^2 V_0[\boldsymbol{\xi}_\alpha]$, the following inequality holds for an arbitrary unbiased estimator $\hat{\boldsymbol{u}}$ of $\boldsymbol{u}$ [7]:

$$V[\hat{\boldsymbol{u}}] \succ \sigma^2 \Big(\sum_{\alpha=1}^{N} \frac{(\boldsymbol{P}_{\mathcal{U}} \bar{\boldsymbol{\xi}}_\alpha)(\boldsymbol{P}_{\mathcal{U}} \bar{\boldsymbol{\xi}}_\alpha)^\top}{(\boldsymbol{u}, V_0[\boldsymbol{\xi}_\alpha]\boldsymbol{u})} \Big)^-_8. \tag{11}$$

Here, $\succ$ means that the left-hand side minus the right is positive semidefinite, and $(\,\cdot\,)^-_r$ denotes the pseudoinverse of rank r. Chernov and Lesort [2] called the right-hand side of Eq. (11) the *KCR* (*Kanatani-Cramer-Rao*) *lower bound* and showed that Eq. (11) holds up to $O(\sigma^4)$ even if $\hat{\boldsymbol{u}}$ is not unbiased; it is sufficient that $\hat{\boldsymbol{u}} \to \boldsymbol{u}$ as $\sigma \to 0$.

Maximum likelihood. If the noise in $\{\boldsymbol{\xi}_\alpha\}$ is independent and Gaussian with mean $\boldsymbol{0}$ and covariance matrix $\sigma^2 V_0[\boldsymbol{\xi}_\alpha]$, *maximum likelihood* (ML) estimation of $\boldsymbol{u}$ is to minimize the sum of square *Mahalanobis distances*

$$J = \sum_{\alpha=1}^{N} (\boldsymbol{\xi}_\alpha - \bar{\boldsymbol{\xi}}_\alpha, V_0[\boldsymbol{\xi}_\alpha]^-_2 (\boldsymbol{\xi}_\alpha - \bar{\boldsymbol{\xi}}_\alpha)), \tag{12}$$

subject to $(\boldsymbol{u}, \bar{\boldsymbol{\xi}}_\alpha) = 0$, $\alpha = 1, ..., N$. Eliminating the constraint by using Lagrange multipliers, we obtain [7]

$$J = \sum_{\alpha=1}^{N} \frac{(\boldsymbol{u}, \boldsymbol{\xi}_\alpha)^2}{(\boldsymbol{u}, V_0[\boldsymbol{\xi}_\alpha]\boldsymbol{u})}. \tag{13}$$

The ML estimator $\hat{\boldsymbol{u}}$ minimizes this subject to $\|\boldsymbol{u}\| = 1$ and $(\boldsymbol{u}^\dagger, \boldsymbol{u}) = 0$.

3 A Posteriori Correction

The a posteriori correction approach first minimizes Eq. (13) without considering the rank constraint and then modifies the resulting solution $\tilde{\boldsymbol{u}}$ so as to satisfy it (Fig. 1(a)). A popular method is to compute the singular value decomposition (SVD) of the computed fundamental matrix and replace the smallest singular value by 0, resulting in a matrix of rank 2 "closest" to the original one in norm [5]. We call this *SVD correction*.

A more sophisticated method is the *optimal correction* [7, 11]. According to the statistical optimization theory [7], the covariance matrix $V[\tilde{\boldsymbol{u}}]$ of the rank unconstrained solution $\tilde{\boldsymbol{u}}$ can be evaluated, so $\tilde{\boldsymbol{u}}$ is moved in the direction of the mostly likely fluctuation implied by $V[\tilde{\boldsymbol{u}}]$ until it satisfies the rank constraint (Fig. 1(a)). The procedure goes as follows [7]:

1. Compute the 9×9 matrices

$$\tilde{\boldsymbol{M}} = \sum_{\alpha=1}^{N} \frac{\boldsymbol{\xi}_\alpha \boldsymbol{\xi}_\alpha^\top}{(\tilde{\boldsymbol{u}}, V_0[\boldsymbol{\xi}_\alpha]\tilde{\boldsymbol{u}})}, \tag{14}$$

   and $V_0[\tilde{\boldsymbol{u}}] = (\boldsymbol{P}_{\tilde{\boldsymbol{u}}}\tilde{\boldsymbol{M}}\boldsymbol{P}_{\tilde{\boldsymbol{u}}})_8^-$, where $\boldsymbol{P}_{\tilde{\boldsymbol{u}}} = \boldsymbol{I} - \tilde{\boldsymbol{u}}\tilde{\boldsymbol{u}}^\top$.
2. Update the solution $\tilde{\boldsymbol{u}}$ as follows ($\tilde{\boldsymbol{u}}^\dagger$ is defined by Eq. (8) for $\tilde{\boldsymbol{u}}$):

$$\tilde{\boldsymbol{u}} \leftarrow N[\tilde{\boldsymbol{u}} - \frac{1}{3}\frac{(\tilde{\boldsymbol{u}}, \tilde{\boldsymbol{u}}^\dagger)V_0[\tilde{\boldsymbol{u}}]\tilde{\boldsymbol{u}}^\dagger}{(\tilde{\boldsymbol{u}}^\dagger, V_0[\tilde{\boldsymbol{u}}]\tilde{\boldsymbol{u}}^\dagger)}]. \tag{15}$$

3. If $(\tilde{\boldsymbol{u}}, \tilde{\boldsymbol{u}}^\dagger) \approx 0$, return $\tilde{\boldsymbol{u}}$ and stop. Else, update the matrix $V_0[\tilde{\boldsymbol{u}}]$ in the form

$$\boldsymbol{P}_{\tilde{\boldsymbol{u}}} = \boldsymbol{I} - \tilde{\boldsymbol{u}}\tilde{\boldsymbol{u}}^\top, \qquad V_0[\tilde{\boldsymbol{u}}] \leftarrow \boldsymbol{P}_{\tilde{\boldsymbol{u}}} V_0[\tilde{\boldsymbol{u}}] \boldsymbol{P}_{\tilde{\boldsymbol{u}}}, \tag{16}$$

   and go back to Step 2.

Before doing this, we need to solve unconstrained minimization of Eq. (13), for which many method exist: the *FNS* (*Fundamental Numerical Scheme*) of Chojnacki et al. [3], the *HEIV* (*Heteroscedastic Errors-in-Variable*) of Leedan and Meer [10], and the *projective Gauss-Newton iterations* of Kanatani and Sugaya [8]. Their convergence properties were studies in [8].

4 Internal Access

The fundamental matrix $\boldsymbol{F}$ has nine elements, on which the normalization $\|\boldsymbol{F}\| = 1$ and the rank constraint $\det \boldsymbol{F} = 0$ are imposed. Hence, it has seven degrees of freedom. The internal access minimizes Eq. (13) by searching the reduced 7-D parameter space (Fig. 1(b)).

Many types of 7-degree parameterizations have been proposed in the past [12, 14], but the resulting expressions are often complicated, and the geometric meaning of the individual unknowns are not clear. This was overcome by Bartoli and Sturm [1], who regarded the SVD of $\boldsymbol{F}$ as its parameterization. Their expression is compact, and each parameter has its geometric meaning. They did tentative 3-D reconstruction using the assumed $\boldsymbol{F}$ and adjusted the reconstructed shape, the camera positions, and their intrinsic parameters so that the reprojection error is minimized; such an approach is known as bundle adjustment. Sugaya and Kanatani [13] simplified this: adopting the parameterization of Bartoli and Sturm [1], they directly minimized Eq. (13) by the Levenberg-Marquardt (LM) method. Their 7-parameter LM search goes as follows:

1. Initialize $\boldsymbol{F}$ in such a way that $\det \boldsymbol{F} = 0$ and $\|\boldsymbol{F}\| = 1$, and express it as $\boldsymbol{F} = \boldsymbol{U}\mathrm{diag}(\cos\theta, \sin\theta, 0)\boldsymbol{V}^\top$.
2. Compute J in Eq. (13), and let $c = 0.0001$.
3. Compute the matrices $\boldsymbol{F}_U$ and $\boldsymbol{F}_V$ and the vector $\boldsymbol{u}_\theta$ as follows:

$$\boldsymbol{F}_U = \begin{pmatrix} 0 & F_{31} & -F_{21} \\ 0 & F_{32} & -F_{22} \\ 0 & F_{33} & -F_{23} \\ -F_{31} & 0 & F_{11} \\ -F_{32} & 0 & F_{12} \\ -F_{33} & 0 & F_{13} \\ F_{21} & -F_{11} & 0 \\ F_{22} & -F_{12} & 0 \\ F_{23} & -F_{13} & 0 \end{pmatrix}, \quad \boldsymbol{F}_V = \begin{pmatrix} 0 & F_{13} & -F_{12} \\ -F_{13} & 0 & F_{11} \\ F_{12} & -F_{11} & 0 \\ 0 & F_{23} & -F_{22} \\ -F_{23} & 0 & F_{21} \\ F_{22} & -F_{21} & 0 \\ 0 & F_{33} & -F_{32} \\ -F_{33} & 0 & F_{31} \\ F_{32} & -F_{31} & 0 \end{pmatrix}, \tag{17}$$

$$\boldsymbol{u}_\theta = \begin{pmatrix} U_{12}V_{12}\cos\theta - U_{11}V_{11}\sin\theta \\ U_{12}V_{22}\cos\theta - U_{11}V_{21}\sin\theta \\ U_{12}V_{32}\cos\theta - U_{11}V_{31}\sin\theta \\ U_{22}V_{12}\cos\theta - U_{21}V_{11}\sin\theta \\ U_{22}V_{22}\cos\theta - U_{21}V_{21}\sin\theta \\ U_{22}V_{32}\cos\theta - U_{21}V_{31}\sin\theta \\ U_{32}V_{12}\cos\theta - U_{31}V_{11}\sin\theta \\ U_{32}V_{22}\cos\theta - U_{31}V_{21}\sin\theta \\ U_{32}V_{32}\cos\theta - U_{31}V_{31}\sin\theta \end{pmatrix}. \tag{18}$$

4. Compute the following matrix $\boldsymbol{X}$:

$$\boldsymbol{X} = \sum_{\alpha=1}^{N} \frac{\boldsymbol{\xi}_\alpha \boldsymbol{\xi}_\alpha^\top}{(\boldsymbol{u}, V_0[\boldsymbol{\xi}_\alpha]\boldsymbol{u})} - \sum_{\alpha=1}^{N} \frac{(\boldsymbol{u}, \boldsymbol{\xi}_\alpha)^2 V_0[\boldsymbol{\xi}_\alpha]}{(\boldsymbol{u}, V_0[\boldsymbol{\xi}_\alpha]\boldsymbol{u})^2}. \tag{19}$$

5. Compute the first and (Gauss-Newton approximated) second derivatives of J as follows:

$$\nabla_{\omega} J = \boldsymbol{F}_U^{\top} \boldsymbol{X} \boldsymbol{u}, \quad \nabla_{\omega'} J = \boldsymbol{F}_V^{\top} \boldsymbol{X} \boldsymbol{u}, \quad \frac{\partial J}{\partial \theta} = (\boldsymbol{u}_{\theta}, \boldsymbol{X} \boldsymbol{u}), \tag{20}$$

$$\nabla_{\omega}^2 J = \boldsymbol{F}_U^{\top} \boldsymbol{M} \boldsymbol{F}_U, \quad \nabla_{\omega'}^2 J = \boldsymbol{F}_V^{\top} \boldsymbol{M} \boldsymbol{F}_V, \quad \nabla_{\omega\omega'} J = \boldsymbol{F}_U^{\top} \boldsymbol{M} \boldsymbol{F}_V,$$
$$\frac{\partial J^2}{\partial \theta^2} = (\boldsymbol{u}_{\theta}, \boldsymbol{M} \boldsymbol{u}_{\theta}), \quad \frac{\partial \nabla_{\omega} J}{\partial \theta} = \boldsymbol{F}_U^{\top} \boldsymbol{M} \boldsymbol{u}_{\theta}, \quad \frac{\partial \nabla_{\omega'} J}{\partial \theta} = \boldsymbol{F}_V^{\top} \boldsymbol{M} \boldsymbol{u}_{\theta}. \tag{21}$$

6. Compute the following matrix $\boldsymbol{H}$:

$$\boldsymbol{H} = \begin{pmatrix} \nabla_{\omega}^2 J & \nabla_{\omega\omega'} J & \partial \nabla_{\omega} J / \partial \theta \\ (\nabla_{\omega\omega'} J)^{\top} & \nabla_{\omega'}^2 J & \partial \nabla_{\omega'} J / \partial \theta \\ (\partial \nabla_{\omega} J / \partial \theta)^{\top} & (\partial \nabla_{\omega'} J / \partial \theta)^{\top} & \partial J^2 / \partial \theta^2 \end{pmatrix}. \tag{22}$$

7. Solve the simultaneous linear equations

$$(\boldsymbol{H} + cD[\boldsymbol{H}]) \begin{pmatrix} \boldsymbol{\omega} \\ \boldsymbol{\omega}' \\ \Delta\theta \end{pmatrix} = - \begin{pmatrix} \nabla_{\omega} J \\ \nabla_{\omega'} J \\ \partial J / \partial \theta \end{pmatrix}, \tag{23}$$

   for $\boldsymbol{\omega}$, $\boldsymbol{\omega}'$, and $\Delta\theta$, where $D[\,\cdot\,]$ denotes the diagonal matrix obtained by taking out only the diagonal elements.
8. Update $\boldsymbol{U}$, $\boldsymbol{V}$, and θ in the form $\boldsymbol{U}' = \mathcal{R}(\boldsymbol{\omega})\boldsymbol{U}$, $\boldsymbol{V}' = \mathcal{R}(\boldsymbol{\omega}')\boldsymbol{V}$, and $\theta' = \theta + \Delta\theta$, where $\mathcal{R}(\boldsymbol{\omega})$ denotes rotation around $N[\boldsymbol{\omega}]$ by angle $\|\boldsymbol{\omega}\|$.
9. Update $\boldsymbol{F}$ to $\boldsymbol{F}' = \boldsymbol{U}' \mathrm{diag}(\cos\theta', \sin\theta', 0) \boldsymbol{V}'^{\top}$.
10. Let J' be the value of Eq. (13) for $\boldsymbol{F}'$.
11. Unless $J' < J$ or $J' \approx J$, let $c \leftarrow 10c$, and go back to Step 7.
12. If $\boldsymbol{F}' \approx \boldsymbol{F}$, return $\boldsymbol{F}'$ and stop. Else, let $\boldsymbol{F} \leftarrow \boldsymbol{F}'$, $\boldsymbol{U} \leftarrow \boldsymbol{U}'$, $\boldsymbol{V} \leftarrow \boldsymbol{V}'$, $\theta \leftarrow \theta'$, and $c \leftarrow c/10$, and go back to Step 3.

5 External Access

The external access approach does iterations in the 9-D $\boldsymbol{u}$-space in such a way that an optimal solution satisfying the rank constraint automatically results (Fig. 1(c)). The concept dates back to such heuristics as introducing penalties to the violation of the constraints or projecting the solution onto the surface of the constraints in the course of iterations, but it is Chojnacki et al. [4] that first presented a systematic scheme, which they called *CFNS* (*Constrained FNS*). Kanatani and Sugaya [9] pointed out, however, that CFNS does not necessarily converge to a correct solution and presented in a more general framework a new scheme, called *EFNS* (*Extended FNS*), which is shown to converge to an optimal value. For fundamental matrix computation, it reduces to the following form:

1. Initialize $\boldsymbol{u}$.
2. Compute the matrix $\boldsymbol{X}$ in Eq. (19).

3. Computer the projection matrix $\boldsymbol{P}_{\boldsymbol{u}^\dagger} = \boldsymbol{I} - \boldsymbol{u}^\dagger \boldsymbol{u}^{\dagger\top}$ ($\boldsymbol{u}^\dagger$ is defined by Eq. (8)).
4. Compute $\boldsymbol{Y} = \boldsymbol{P}_{\mathbf{u}^\dagger} \boldsymbol{X} \boldsymbol{P}_{\mathbf{u}^\dagger}$.
5. Solve the eigenvalue problem $\boldsymbol{Y}\boldsymbol{v} = \lambda \boldsymbol{v}$, and compute the two unit eigenvectors $\boldsymbol{v}_1$ and $\boldsymbol{v}_2$ for the smallest eigenvalues in absolute terms.
6. Compute $\hat{\boldsymbol{u}} = (\boldsymbol{u}, \boldsymbol{v}_1)\boldsymbol{v}_1 + (\boldsymbol{u}, \boldsymbol{v}_2)\boldsymbol{v}_2$.
7. Compute $\boldsymbol{u}' = N[\boldsymbol{P}_{\mathbf{u}^\dagger} \hat{\boldsymbol{u}}]$.
8. If $\boldsymbol{u}' \approx \boldsymbol{u}$, return $\boldsymbol{u}'$ and stop. Else, let $\boldsymbol{u} \leftarrow N[\boldsymbol{u} + \boldsymbol{u}']$ and go back to Step 2.

6 Bundle Adjustment

The transition from Eq. (12) to Eq. (13) is *exact*; no approximation is involved. Strictly speaking, however, the minimization of the (squared) Mahalanobis distance in the $\boldsymbol{\xi}$-space (Eq. (13)) can be ML only when the noise in the $\boldsymbol{\xi}$-space is Gaussian, because then and only then is the likelihood proportional to $e^{-J/\text{constant}}$. If the noise in the image plane is Gaussian, on the other hand, the transformed noise in the $\boldsymbol{\xi}$-space is no longer Gaussian, so minimizing Eq. (13) is not strictly ML in the image plane. In order to test how much difference is incurred, we also implemented bundle adjustment, minimizing the reprojection error (we omit the details).

7 Experiments

Figure 2 shows simulated images of two planar grid surfaces viewed from different angles. The image size is 600×600 pixels with 1200 pixel focal length. We added random Gaussian noise of mean 0 and standard deviation σ to the x- and y-coordinates of each grid point independently and from them computed the fundamental matrix by 1) SVD-corrected LS, 2) SVD-corrected ML, 3) CFNS, 4) optimally corrected ML, 5) 7-parameter LM, and 6) EFNS.

"LS" means least squares (also called "8-point algorithm" [5]) minimizing $\sum_{\alpha=1}^{N} (\boldsymbol{u}, \boldsymbol{\xi}_\alpha)^2$, which reduces to simple eigenvalue computation [8]. For brevity,

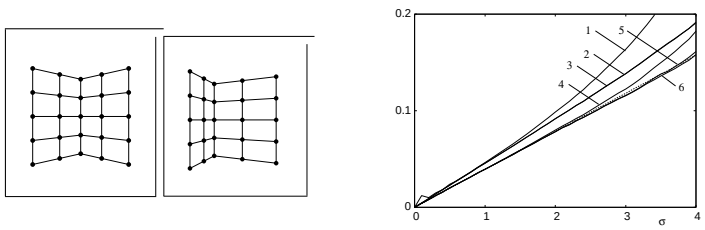

Fig. 2. Simulated images of planar grid surfaces and the RMS error vs. noise level. 1) SVD-corrected LS. 2) SVD-corrected ML. 3) CFNS. 4) Optimally corrected ML. 5) 7-parameter LM. 6) EFNS. The dotted line indicates the KCR lower bound.

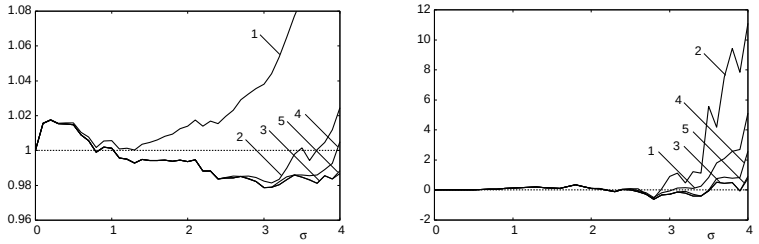

(a) (b)

Fig. 3. (a) The RMS error relative to the KCR lower bound. (b) Average residual minus minus $(N-7)\sigma^2$. 1) Optimally corrected ML. 2) 7-parameter LM started from LS. 3) 7-parameter LM started from optimally corrected ML. 4) EFNS. 5) Bundle adjustment.

we use the shorthand "ML" for unconstrained minimization of Eq. (13), for which we used the FNS of Chojnacki et al. [3]. The 7-parameter LM and CFNS are initialized by LS. All iterations are stopped when the update of $\boldsymbol{F}$ is less than 10^{-6} in norm.

On the right of Fig. 2 is plotted for σ on the horizontal axis the following root-mean-square (RMS) error D corresponding to Eq. (7) over 10000 independent trials:

$$D = \sqrt{\frac{1}{10000}\sum_{a=1}^{10000} \|\boldsymbol{P}_{\mathcal{U}}\hat{\boldsymbol{u}}^{(a)}\|^2}. \tag{24}$$

Here, $\hat{\boldsymbol{u}}^{(a)}$ is the ath value, and $\boldsymbol{P}_{\mathcal{U}}$ is the projection matrix in Eq. (10). The dotted line is the bound implied by the KCR lower bound (the trace of the right-hand side of Eq. (11)).

Preliminary observations. We can see that SVD-corrected LS (Hartley's 8-point algorithm) performs very poorly. We can also see that SVD-corrected ML is inferior to optimally corrected ML, whose accuracy is close to the KCR lower bound. The accuracy of the 7-parameter LM is nearly the same as optimally corrected ML when the noise is small but gradually outperforms it as the noise increases. Best performing is EFNS, exhibiting nearly the same accuracy as the KCR lower bound. In contrast, CFNS performs as poorly as SVD-corrected ML. The reason for this is fully investigated by Kanatani and Sugaya [9].

Doing many experiments (not all shown here), we have observed that i) EFNS stably achieves the highest accuracy over a wide range of the noise level, ii) optimally corrected ML is fairly accurate and very robust to noise but gradually deteriorates as noise grows, and iii) 7-parameter LM achieves very high accuracy when started from a good initial value but is likely to fall into local minima if poorly initialized.

The robustness of EFNS and optimally corrected ML is due to the fact that the computation is done in the redundant ("external") $\boldsymbol{u}$-space, where J has a simple form of Eq. (13). In fact, we have never experienced local minima in our

	residual	time
1	45.550	.000524
2	45.556	.00652
3	45.556	.01300
4	45.378	.00764
5	45.378	.01136
6	45.378	.01748
7	45.379	.01916
8	45.379	.02580

Fig. 4. Left: Real images and 100 corresponding points. Right: Residuals and execution times (sec) for 1) SVD-corrected LS, 2) SVD-corrected ML, 3) CFNS, 4) optimally corrected ML, 5) direct search from LS, 6) direct search from optimally corrected ML, 7) EFNS, 8) bundle adjustment.

experiments. The deterioration optimally corrected ML in the presence of large noise is because linear approximation is involved in Eq. (15).

The fragility of 7-parameter LM is attributed to the complexity of the function J when expressed in seven parameters, resulting in many local minima in the reduced ("internal") parameter space, as pointed out in [12].

Thus, the optimal correction of ML and the 7-parameter ML have complementary characteristics, which suggests that the 7-parameter ML initialized by optimally corrected ML may exhibit comparable accuracy to EFNS. We now confirm this.

Detailed observations. Figure 3(a) compares 1) optimally corrected ML, 2) 7-parameter LM started from LS, 3) 7-parameter LM started from optimally corrected ML, 4) EFNS, and 5) bundle adjustment. For visual ease, we plot the ratio $D/D_{\rm KCR}$ of D in Eq. (24) to the corresponding KCR lower bound. Figure 3(b) plots the corresponding average residual J (minimum of Eq. (13). Since direct plots of J nearly overlap, we plot its difference from $(N-7)\sigma^2$, where N is the number of corresponding pairs. This is motivated by the fact that to a first approximation $\hat{J}/\sigma^2$ is subject to a χ^2 distribution with $N-7$ degrees of freedom [7], so the expectation of $\hat{J}$ is approximately $(N-7)\sigma^2$.

We observe from Fig. 3 that i) the RMS error of optimally corrected ML increases as noise increases, *yet* the corresponding residual remains low, ii) the 7-parameter LM started from LS appears to have high accuracy for noise levels for which the corresponding residual high, iii) the accuracy of the 7-parameter LM improves if started from optimally corrected ML, resulting in the accuracy is comparable to EFNS, and iv) additional bundle adjustment does *not* increase the accuracy to any noticeable degree.

The seeming contradiction that solutions that are closer to the true value (measured in RMS) have *higher residuals* $\hat{J}$ implies that the 7-parameter LM failed to reach the true minimum of the function J, indicating existence of local minima located close to the true value. When initialized by the optimally corrected ML, the 7-parameter LM successfully reaches the true minimum of J, resulting in the smaller $\hat{J}$ but *larger* RMS errors.

Real image example. We manually selected 100 pairs of corresponding points in the two images in Fig. 4 and computed the fundamental matrix from them.

The final residual J and the execution time (sec) are listed there. We used Core2Duo E6700 2.66GHz for the CPU with 4GB main memory and Linux for the OS.

We can see that for this example optimally corrected ML, 7-parameter LM started from either LS or optimally corrected ML, EFNS, and bundle adjustment all converged to the same solution, indicating that all are optimal. On the other hand, SVD-corrected LS (Hartley's 8-point method) and SVD-corrected ML have higher residual than the optimal solution and that CFNS has as high a residual as SVD-corrected ML.

8 Conclusions

We compared algorithms for fundamental matrix computation (the source code is available from the authors' Web page[1]), which we classified into "a posteriori correction", "internal access", and "external access".

We observed that the popular SVD-corrected LS (Hartley's 8-point algorithm) has poor performance and that the CFNS of Chojnacki et al. [4], a pioneering external access method, does not necessarily converge to a correct solution, while the EFNS always yields an optimal value.

After many experiments (not all shown here), we concluded that EFNS and the 7-parameter LM started from optimally corrected ML exhibited the best performance. We also observed that additional bundle adjustment does not increase the accuracy to any noticeable degree.

Acknowledgments: This work was done in part in collaboration with Mitsubishi Precision, Co. Ldt., Japan. The authors thank Mike Brooks, Wojciech Chojnacki, and Anton van den Hengel of the University Adelaide, Australia, for providing software and helpful discussions. They also thank Nikolai Chernov of the University of Alabama at Birmingham, U.S.A. for helpful discussions.

References

1. Bartoli, A., Sturm, P.: Nonlinear estimation of fundamental matrix with minimal parameters. IEEE Trans. Patt. Anal. Mach. Intell. 26(3), 426–432 (2004)
2. Chernov, N., Lesort, C.: Statistical efficiency of curve fitting algorithms, Comput. Stat. Data Anal. 47(4), 713–728 (2004)
3. Chojnacki, W., Brooks, M.J., van den Hengel, A., Gawley, D.: On the fitting of surfaces to data with covariances, IEEE Trans. Patt. Anal. Mach. Intell. 22(11), 1294–1303 (2000)
4. Chojnacki, W., Brooks, M.J., van den Hengel, A., Gawley, D.: A new constrained parameter estimator for computer vision applications, Image Vis. Comput. 22(2), 85–91 (2004)
5. Hartley, R.I.: In defense of the eight-point algorithm, IEEE Trans. Patt. Anal. Mach. Intell. 19(6), 580–593 (1997)

[1] http://www.iim.ics.tut.ac.jp/~sugaya/public-e.html

6. Hartley, R., Zisserman, A.: Multiple View Geometry in Computer Vision Cambridge University Press, Cambridge, U.K. (2000)
7. Kanatani, K.: Statistical Optimization for Geometric Computation: Theory and Practice Elsevier Science, Amsterdam, The Netherlands, 1996; Dover, New York (2005)
8. Kanatani, K., Sugaya, Y.: High accuracy fundamental matrix computation and its performance evaluation, In: Proc. 17th British Machine Vision Conf., Edinburgh, UK, September 2006, vol. 1, pp. 217–226 (2006)
9. Kanatani, K., Sugaya, Y.: Extended FNS for constrained parameter estimation, In: Proc. 10th Meeting Image Recog. Understand., Hiroshima, Japan, July 2007, pp. 219–226 (2007)
10. Leedan, Y., Meer, P.: Heteroscedastic regression in computer vision: Problems with bilinear constraint, Int. J. Comput. Vision. 37(2), 127–150 (2000)
11. Matei, J., Meer, P.: Estimation of nonlinear errors-in-variables models for computer vision applications, IEEE Trans. Patt. Anal. Mach. Intell. 28(10), 1537–1552 (2006)
12. Migita, T., Shakunaga, T.: One-dimensional search for reliable epipole estimation, In: Proc. IEEE Pacific Rim Symp. Image and Video Technology, Hsinchu, Taiwan, December 2006, pp. 1215–1224 (2006).
13. Sugaya, Y., Kanatani, K.: High accuracy computation of rank-constrained fundamental matrix, In: Proc. 18th British Machine Vision Conf., Coventry, UK, September 2007, vol. 1, pp. 282–291 (2007)
14. Zhang, Z., Loop, C.: Estimating the fundamental matrix by transforming image points in projective space, Comput. Vis. Image Understand. 82(2), 174–180 (2001)